PHYSICAL REVIEW D VOLUME 20, NUMBER 1 1 JULY 1979

Kinematics-free angular momentum trajectories. I. Theory and phenomenology

Robert A. Leacock
Ames Laboratory, United States Department of Energy and Department of Physics, Iowa State University, Ames, Iowa 50011
(Received 8 December 1975)

In the main part of this paper it is shown how to define other complex angular momentum trajectories which are related to, but distinct from, the usual Regge trajectory α. One of these other trajectories, called here γ, is a zero of a function Y (which is essentially the cotangent of the scattering phase shift for *physical* values of the angular momentum) in contrast to the Regge trajectory α which is a zero of the inverse S matrix. γ has simpler analyticity properties as a function of energy than α. The γ trajectory is, in one sense, the α trajectory with the contribution of the elastic kinematics removed; thus γ is real between the elastic threshold and the inelastic threshold, unlike α. The ways by which γ and α produce bound states and elastic and inelastic resonances are compared and contrasted. One unusual feature of the γ trajectory is that it can be purely real and still produce resonances of finite width. In the secondary part of the paper the pion-nucleon elastic-phase-shift "data" of the P_{33} and F_{37} partial waves in the regions of the $P_{33}(1232)$ and $F_{37}(1950)$ resonances are given a direct-channel complex angular momentum interpretation using a crude model based on the γ trajectory. The model fitted to the data (1) provides an illustration of the use of the γ trajectory, and (2) demonstrates the feasibility of a direct-channel complex angular momentum analysis of scattering data.

I. INTRODUCTION

Despite the extensive theoretical and phenomenological applications of the concept of a complex angular momentum trajectory to problems in particle physics,[1-5] the concept, so far, has not found detailed phenomenological application in the direct channel.[3,5] The cross-channel applications, of which the interpretation of pion-nucleon charge-exchange scattering using ρ-trajectory exchange is perhaps the cleanest, are numerous and detailed. The classification of particles (bound states and resonances) by angular momentum trajectories can, perhaps, be called a direct-channel application of the idea of a complex angular momentum pole, however, the connection in this application between the theory and the data is tenuous at best. For example, the imaginary part of the trajectory rarely plays a role here. It was the desire to give the concept of a complex angular momentum trajectory a careful test in the direct channel that formed the initial motivation for the present study.

There are two main reasons why a direct-channel phenomenological analysis proceeds most naturally in terms of partial-wave amplitudes. First, a given complex angular momentum (Regge) pole of the amplitude contributes only to some, and not to all, of the partial-wave amplitudes. Thus the contributions of the various trajectories are partially disentangled by considering the partial waves; one need only consider the one or two Regge poles that contribute to a given wave in the energy region studied. Second, in the past few years excellent partial-wave analyses of low-energy strongly interacting systems have become available; the most notable example is perhaps the pion-nucleon elastic-phase-shift analyses where there are a number of detailed analyses in substantial agreement over their wide energy regions (from threshold to above 2200 MeV).[6-10]

While the isolation of Regge-pole contributions and the availability of good phase-shift analyses are strong advantages to doing a direct-channel complex angular momentum interpretation of scattering data in terms of partial waves, there are some well-known disadvantages. The two most outstanding, and connected, disadvantages are that "Reggeized" partial-wave amplitudes in general (1) do not obey naturally elastic unitarity, and (2) do not have the correct energy dependence at threshold.[2,3,11] Examination of these points is especially important in, e.g., the πN P_{33} wave near threshold which is also the region of the 1232-MeV resonance. Proper treatment of unitarity and threshold behavior is essential in studying this elastic resonance.

Many of the above problems are most easily solved by constructing complex angular momentum models of a function Y which is essentially the cotangent of the scattering phase shift for *physical* values of the angular momentum. The main result of this paper is the observation that a complex angular momentum model of the function Y (and thus of the partial-wave amplitude) is naturally accomplished in terms of a different complex angular momentum trajectory than the usual Regge trajectory α. This new trajectory, called here γ, is a zero of the function Y, while α is a zero of

the inverse S matrix (or of the inverse amplitude). The main purpose of the present paper is to define and illustrate the γ trajectory; the secondary purpose is to show that a direct-channel complex angular momentum interpretation of low-energy πN partial-wave amplitudes is possible.

In Sec. II γ and α trajectories are defined, while in Sec. III the production of bound states and resonances by γ and α trajectories is discussed. Section IV is devoted to a brief discussion of the analytic properties and formal relationship of the γ and α trajectories, while Sec. V is a phenomenological illustration of the γ trajectory using the πN P_{33} and F_{37} partial waves in the regions of the 1232 and 1950 MeV resonances, respectively. Section VI contains six observations about the γ and α complex angular momentum trajectories.

II. DEFINITION OF ANGULAR MOMENTUM TRAJECTORIES

The partial-wave amplitude for the elastic scattering of two spinless particles of mass m is[12]

$$A(\nu,l)=(e^{2i\delta(\nu,l)}-1)/2i\nu^{1/2}, \tag{1}$$

where q is the magnitude of the center-of-mass-system (c.m.s.) three-momentum, $\nu=q^2$, $s=4(\nu+m^2)$ is the total c.m.s. energy squared, l is the orbital angular momentum index, and δ is the usual phase shift, real for elastic scattering. [The notation follows BZ except for the suppression of (1) a factor $(\nu+m^2)^{1/2}$ in Eq. (1), and in subsequent equations for $A(\nu,l)$, and (2) a signature superscript on $A(\nu,l)$.] BZ show that Eq. (1) may be rewritten as

$$A(\nu,l)=\frac{\nu^l\cos\pi l}{Y(\nu,l)+(-\nu)^{l+1/2}}, \tag{2}$$

where by $(-\nu)^{l+1/2}$ is meant $\exp[(l+\frac{1}{2})\ln(-\nu-i\epsilon)]$. The function $Y(\nu,l)$ is $\pm\nu^{l+1/2}\cot\delta(\nu,l)$ for *physical* values of l. Equation (2) may be taken as defining $Y(\nu,l)$. The properties of $Y(\nu,l)$ follow from the Mandelstam representation in a relativistic treatment,[3,12] or from the radial Schrödinger equation in a nonrelativistic discussion.[1] In either case Y is a real meromorphic function of ν and l which contains no elastic cut, i.e., in the ν plane Y has a left-hand cut and a right-hand cut beginning at the inelastic threshold ($\nu=\nu_{\text{inel}}$) instead of at the elastic threshold ($\nu=0$) where the right-hand cut of $A(\nu,l)$ begins. In the sense that the elastic kinematics have been "removed" in $Y(\nu,l)$, it is a "purely dynamical function" (see, however, Sec. III).

Since the Regge poles are poles in the complex l plane of amplitude (2), it is useful to define a denominator function $D(\nu,l)$ by

$$D(\nu,l)\equiv Y(\nu,l)+(-\nu)^{l+1/2} \tag{3}$$

in terms of which the usual Regge trajectory $\alpha(\nu)$ is defined by

$$D(\nu,\alpha(\nu))=Y(\nu,\alpha(\nu))+(-\nu)^{\alpha(\nu)+1/2}=0. \tag{4}$$

This definition of the trajectory $\alpha(\nu)$ contains, roughly speaking, a "dynamical" function Y and a "kinematical" function $(-\nu)^{l+1/2}$, thus one might expect $\alpha(\nu)$ to contain such a mixture. In order to remove the elastic kinematics from the angular momentum trajectory, one may modify definition (4) by eliminating the so-called kinematic term $(-\nu)^{l+1/2}$. This procedure defines a "kinematics-free" or "reduced" angular momentum trajectory $\gamma(\nu)$ by

$$Y(\nu,\gamma(\nu))=0. \tag{5}$$

The trajectories $\alpha(\nu)$ and $\gamma(\nu)$ are closely related; an exact relation is given in Sec. IV.

Alternatively to being a zero of $D(\nu,l)$, the Regge trajectory $\alpha(\nu)$ may be viewed as a pole of the amplitude $A(\nu,l)$ or of the S matrix: $S(\nu,l)\equiv\exp[2i\delta(\nu,l)]$. Correspondingly, the γ trajectory may be viewed as the pole of a sort of "reduced amplitude" $Y^{-1}(\nu,l)$. De Alfaro and Regge remark on page forty of their book[1] that the introduction of the function Y "simplifies drastically the description of the analytic properties of" the S matrix because of the analytic properties of Y as a function of ν. In summary, Eqs. (4) and (5) will be used throughout this paper to define the α and γ trajectories, respectively.

Using the phase shift and K matrix in a potential-scattering formalism, Tani and Inokuti[13] define a "maximal-amplitude trajectory"; the relation between their concept and the α and γ trajectories is discussed in Appendix A.

The properties and relationship of γ and α are discussed in some detail below; at this point it is only remarked that the γ trajectory does not have the right-hand "kinematic" cut in the ν plane that the α trajectory has (see Sec. IV).

III. BOUND STATES AND RESONANCES

Although the complex angular momentum function $\gamma(\nu)$ does not trace out the same trajectory in the complex l plane as does $\alpha(\nu)$, it nevertheless "produces" resonances and bound states in the same manner: by passing close to, or through, a physical (integer ≥ 0) value of l. Furthermore, the γ trajectory groups bound states and resonances into families as does the Regge trajectory α.

A. Resonances

The simplest expression for a resonating amplitude is the familiar Breit-Wigner form A

$= (\nu^{-1/2} M_0 \Gamma x)/(s_0 - s - iM_0\Gamma)$, where M_0 is the resonance mass, $s_0 = M_0^2$, $\Gamma(\nu) = \Gamma_0(\nu/\nu_0)^{l+1/2}$, where Γ_0 is the resonance width, ν_0 is defined by $s_0 = 4(\nu_0 + m^2)$, and where x is the resonance elasticity. The resonance parameters M_0, Γ_0, and x are here assumed real constants in the vicinity of a resonance, they may, of course, be functions of the index l. The corresponding complex angular momentum expressions are derived as follows. Since γ and α are zeros of Y and D, respectively, one can define "residue" functions H and W by

$$\begin{aligned} Y(\nu, l) &\equiv [l - \gamma(\nu)]H, \\ D(\nu, l) &\equiv [l - \alpha(\nu)]W, \end{aligned} \tag{6}$$

where, in the most general case, H is a function of ν, l, $\gamma(\nu)$, W is a function of ν, l, $\alpha(\nu)$. In the vicinity of a resonance of energy s_0, angular momentum l, the trajectory functions γ and α are expanded

$$\begin{aligned} \gamma(\nu) &= l + \gamma_R'(s - s_0) + \cdots + i\gamma_I, \\ \alpha(\nu) &= l + \alpha_R'(s - s_0) + \cdots + i\alpha_I. \end{aligned} \tag{7}$$

H is, for convenience only, assumed real: $H = H_R$. Under these assumptions use of (6) and (7) in (3) and (2) yields near $s = s_0$

$$A(\nu, l) \simeq \frac{\nu^l/\gamma_R' H_R}{(s_0 - s) - i(\gamma_I + \nu^{l+1/2}/H_R)/\gamma_R'}, \tag{8}$$

$$A(\nu, l) \simeq \frac{\nu^l/\alpha_R' W}{(s_0 - s) - i\alpha_I/\alpha_R'}. \tag{9}$$

In these formulas l is an even integer (for l an odd integer, several minus signs appear in the formulas; these are not important for the present discussion). Comparison of Eqs. (8) and (9) with the Breit-Wigner form indicates immediately the connections between the resonance parameters and the complex angular momentum functions. The elastic and inelastic cases are discussed separately.

For the elastic case ($\nu < \nu_{\text{inel}}$) where $x = 1$ the function $Y(\nu, l)$ is real, and, via Eq. (6), one may take $\gamma(\nu)$ and H real (see Sec. IV). Thus $\gamma_I = 0$, however, the resonance still has a finite width since from (8)

$$M^0\Gamma(\nu) = \nu^{l+1/2}/\gamma_R' H_R,$$

which is to be compared to the usual Regge result from (9)

$$M^0\Gamma(\nu) = \alpha_I/\alpha_R'. \tag{10}$$

Thus the γ trajectory produces resonances of finite width in the elastic region where it is a purely real function. In this region the α trajectory has, of course, a nonzero imaginary part as seen, e.g., in Eq. (10). As will be discussed below, γ passes through the point l in the angular momentum plane, while α passes near it.

In the inelastic region ($\nu > \nu_{\text{inel}}$) where $x < 1$, in general Y and γ are complex. Equation (8) now yields

$$M^0\Gamma(\nu) = (\gamma_I + \nu^{l+1/2}/H_R)/\gamma_R', \tag{11}$$

which more closely resembles (10). In this region, since $\gamma_I \neq 0$ in general, the γ trajectory, like the α trajectory, does not pass through the point l, but rather passes close by it, again producing a resonance. The inverse of Eq. (11) is

$$M^0\Gamma(\nu)(1 - x) = \gamma_I/\gamma_R'$$

which, when compared to (10), emphasizes the similarity of γ and α except for the modification in the elastic region where $x = 1$.

The production of resonances by the γ and α trajectories is shown schematically in Fig. 1(a). The γ trajectory produces elastic resonances of angular momentum $l = 2$, 3 by passing *through* the points $l = 2$, 3, while α produces the same resonances by passing *close to* $l = 2$, 3. Above the inelastic threshold, γ and α both produce inelastic resonances of angular momentum $l = 4$, 5, ... until finally they wander too far from the Rel axis to cause resonances.

B. Bound states

If the two-particle system under consideration possesses bound states these will appear, e.g., as poles of the amplitude. In the usual Regge interpretation of these states the trajectory $\alpha(\nu)$ has the value of the bound-state angular momentum at the bound-state energy causing a zero in the denominator of the amplitude.[1-4] Consider a bound state of angular momentum l and three-momentum squared ν'; from Eqs. (3) and (6) the values of the trajectories at the bound state ν' are

$$\begin{aligned} \gamma(\nu') &= l + |\nu'|^{l+1/2}/H, \\ \alpha(\nu') &= l, \end{aligned} \tag{12}$$

where H is real and is evaluated at ν', l. These equations show that α has the value l at $\nu = \nu'$, but that γ "misses" l by an amount $|\nu'|^{l+1/2}/H$. Thus the trajectory γ does not take on the physical angular momentum values at the bound-state energies as does α. Since the discrepancy between γ and l is proportional to the so-called kinematic term $(-\nu)^{l+1/2}$, this casts doubt on the appropriateness of the designation "kinematic-free" used for γ in Sec. II; this is discussed more below.

In Fig. 1(a) is shown γ and α trajectories which produce bound states of angular momentum $l = 0$, 1. Although the paths of γ and α are the same in the

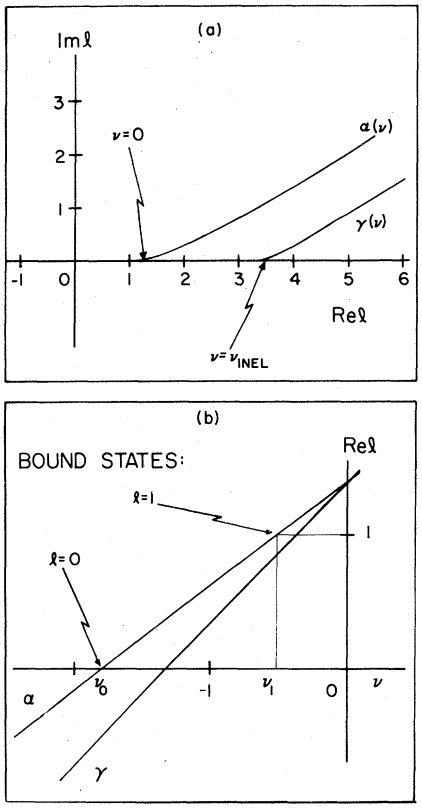

FIG. 1. (a) The complex angular momentum plane showing α and γ trajectories (schematically). The α trajectory leaves the Rel axis at the elastic threshold ($\nu=0$), while the γ trajectory leaves the Rel axis at the inelastic threshold ($\nu=\nu_{\text{inel}}$). Both trajectories "cause" bound states at $l=0$, 1, elastic resonances at $l=2$, 3, and inelastic resonances at $l=4$, 5,..., Note that the γ trajectory is purely real where it produces the elastic $l=2$ and $l=3$ resonances; in spite of this these resonances have a finite width (see text). (b) The α and γ trajectories plotted versus ν below the elastic threshold ($\nu=0$) where both trajectories are real. Both trajectories "cause" the two bound states: $l=1$ at $\nu=\nu_1$ and $l=0$ at $\nu=\nu_0$. Note that α has the bound-state angular momentum at the corresponding bound-state energy, while γ does not, i.e., $\alpha(\nu_1)=1$, $\alpha(\nu_0)=0$, but $\gamma(\nu_1)<1$, $\gamma(\nu_0)<0$. (This figure is drawn for the case where $H<0$ so that $\gamma<\alpha$ for $\nu<0$; see text.)

l plane immediately below the elastic threshold they are not at the same l point for the same ν as was seen, e.g., in Eq. (12). This is shown more clearly in Fig. 1(b) where γ and α are plotted (schematically) versus ν for $\nu<0$. It is clear that γ and α do not have the same value, in general, anywhere in this region (except possibly at $\nu=0$), and in particular, that γ does not have the bound-state l value at the bound-state energy. (The left-hand-cut region farther below threshold is not considered here.)

C. Comparison of γ,α

The complementarity of the γ and α trajectories with respect to the production of bound states and resonances may be summarized as follows. The discussion of Secs. III A and III B plus inspection of Eq. (2) suggests, for purposes of illustration, the following *provisional* definitions of bound states and resonances (ν' real, l integer ≥ 0): bound state at $\nu'<0$, angular momentum l:

$$D(\nu', l)=0\,, \tag{13a}$$

elastic resonance at $\nu'>0$ ($x=1$, Y real):

$$Y(\nu', l)=0\,, \tag{13b}$$

inelastic resonance at $\nu'>0$ ($x<1$, Y complex):

$$D_R(\nu', l)=Y_R(\nu', l)=0 \tag{13c}$$

where the subscript R means real part. The first of Eqs. (13) can also be thought of as following from Eqs. (6) and (12), while the second also follows from (6), (7), and (8). The third of Eqs. (13) is not nearly as clean as the first two, and indeed is very crude.

Using definitions (13) and Eqs. (3) and (6), one constructs the values of the trajectories at the bound state and resonance energies; these are given in Table I. The entries for the bound states and elastic resonances show the complementary relationship of γ and α: In the complex l plane γ is displaced from the bound-state l value for bound states and is exactly the resonance l value for elastic resonances, while α is exactly the bound-state l value for bound states and is displaced from the resonance l value for elastic resonances. Above the inelastic threshold both γ and α are displaced from the inelastic resonance l value for inelastic resonances, although not by the same amount. The entries of Table I are also shown graphically in Fig. 1.

IV. PROPERTIES AND RELATIONSHIP OF γ,α

A. Analyticity, threshold behavior

By the implicit function theorem the domain of analyticity of $\gamma(\nu)$ follows from that of $Y(\nu,l)$, just as the domain of analyticity of $\alpha(\nu)$ follows from that of $D(\nu,l)$, i.e., γ is a real analytic function of ν with right-hand cut beginning at ν_{inel} instead of at $\nu=0$ where the right-hand cut of α begins.[3,14,15] (In this sense γ is "kinematics-free" or "reduced" with, however, the reservations mentioned in Sec. III.) Thus, one expects $\gamma(\nu)$ to be a real function of ν below ν_{inel}, especially between $\nu=0$ and $\nu=\nu_{\text{inel}}$. Exceptions to this expectation of a real γ occur if two γ trajectories collide and "bounce off" into the complex l plane.

TABLE I. Trajectory values at bound states and resonances.

Trajectory[a] \ State at ν', l	Bound state $\nu' < 0$	Elastic resonance $0 < \nu' < \nu_{\text{inel}}$	Inelastic resonance $\nu_{\text{inel}} < \nu'$
$\gamma(\nu') =$	$l + (-\nu')^{l+1/2}/H$	l	$l - iY_I/H$
$\alpha(\nu') =$	l	$l - (-\nu')^{l+1/2}/W$	$l - [iY_I + (-\nu')^{l+1/2}]/W$

[a] H and W are evaluated at ν', l where ν' is real and where l is an integer. $Y_I \equiv \text{Im} Y(\nu', l)$.

The energy regions where $\gamma(\nu)$ is real are examined in more detail in Appendix B.

Because the function $Y(\nu, l)$ does not require a cut in the ν plane at threshold, the γ trajectory has simpler threshold behavior than the α trajectory. Following BZ one defines the real numbers $A_\gamma \equiv \partial Y/\partial \nu$ and $B_\gamma \equiv \partial Y/\partial l$, where the derivatives are evaluated at threshold; $\nu = 0$, $l = \gamma(0)$. Similar numbers obtain for the α trajectory: A_α, β_α. By expansion of $Y(\nu, l)$ and $D(\nu, l)$ about threshold and using the definitions (4), (5) one has the trajectory behavior at threshold:

$$\begin{aligned} \gamma(\nu) &= \gamma(0) - (A_\gamma/B_\gamma)\nu + \cdots , \\ \alpha(\nu) &= \alpha(0) - (A_\alpha/B_\alpha)\nu + \cdots - B_\alpha^{-1}(-\nu)^{\alpha+1/2} . \end{aligned} \tag{14}$$

The "kinematic" term $(-\nu)^{\alpha+1/2}$ produces the imaginary part of $\alpha(\nu)$ immediately above $\nu = 0$; $\gamma(\nu)$ does not have this term and is real immediately above and below threshold. Further, it is clear that, e.g., γ could be linear in ν near threshold, while α cannot be because of the kinematic term.

B. Relationship of γ, α

The trajectories $\gamma(\nu)$ and $\alpha(\nu)$ are two members of a family of trajectories related by a common definition. Defining a generalized denominator function $D(\nu, l, \Lambda)$ by

$$D(\nu, l, \Lambda) \equiv Y(\nu, l) + \Lambda(-\nu)^{l+1/2} , \tag{15}$$

one obtains a generalized trajectory function $\alpha(\nu, \Lambda)$ from the definition

$$D(\nu, \alpha(\nu, \Lambda), \Lambda) = 0 . \tag{16}$$

The γ and α trajectories are thus the special cases

$$\gamma(\nu) = \alpha(\nu, 0) , \quad \alpha(\nu) = \alpha(\nu, 1) .$$

In these expressions Λ is a complex number or, perhaps, a function of some other independent variable. It is clear that the threshold behavior of $\alpha(\nu, \Lambda)$ is just that of $\alpha(\nu)$ with a Λ in front of the $(-\nu)^{\alpha+1/2}$ term [see (14)].

The connection between the members of the continuous family of trajectories defined by (15) and (16) can also be expressed formally in terms of a translation through the distance a in the Λ plane

$$\alpha(\nu, \Lambda + a) = e^{a\partial/\partial\Lambda} \alpha(\nu, \Lambda) .$$

Thus, given the generalized trajectory function and all its Λ derivatives at one point in the Λ plane, the trajectory can be constructed for other Λ.

In conclusion, one observes that the γ trajectory is a rather special member of the family $\alpha(\nu, \Lambda)$, namely $\alpha(\nu, 0)$; this is the only member of the family in which the kinematic term is entirely absent.

V. PION-NUCLEON PHENOMENOLOGY

As an illustration of the general phenomenological character of the γ trajectory, a γ-trajectory model is fitted to the P_{33} and F_{37} partial waves of the pion-nucleon system. The model and the fit, which are crude, are intended only as an illustration of the γ trajectory, and not as a definitive example of a complex angular momentum interpretation of empirical pion-nucleon partial wave amplitudes.

A. P_{33}, F_{37} πN data

Two recent, detailed, and widely available πN partial-wave analyses are the CERN and Saclay studies, called ALMEHED 72 and AYED 73 (or 74), respectively, by the Particle Data Group.[6-10] These analyses are in agreement in their general features. For definiteness, I use the AYED 73 analysis, comparing it to ALMEHED 72 to estimate errors. Only the P_{33} and F_{37} waves are fitted, and, as discussed below, these waves are considered only in the regions of the P_{33} (1232) and F_{37} (1950) resonances, respectively, i.e., only the first two Regge recurrences of the Δ_δ trajectory are examined.

Since the γ trajectory is most closely related to the function $Y(\nu, l)$, one needs to "construct" this function from the data. This is done using the equations (l an odd integer)

$$\begin{aligned} Y^R(\nu, l) &= -\nu^{l+1/2} \cot\Delta(\nu, l) , \\ \Delta(\nu, l) &\equiv \delta(\nu, l) + i\delta'(\nu, l) , \\ \eta(\nu, l) &\equiv \exp[-2\delta'(\nu, l)] , \end{aligned} \tag{17}$$

which follow from Eqs. (1) and (2) for the more general case where the real phase shift δ becomes the complex phase shift Δ. η is the usual absorption parameter. The superscript D on Y^D indicates that Y is "constructed" from the data. Using the AYED 73 phase shifts (δ) and absorptions (η) in Eqs. (17), one constructs the real and imaginary parts of $Y^D(\nu,l)$ for the discrete, physical energies and angular momenta available in the phase-shift analysis. In Fig. 2 these Y^D values are shown as data points versus the total c.m.s. energy squared s for $l=1$ (P_{33} wave near $s=1.5$ GeV^2) and $l=3$ (F_{37} wave near $s=3.8$ GeV^2). The data selected were those points available from the AYED 73 analysis in energy regions with boundaries given by the resonance energy plus and minus the resonance half-width.[10]

Before discussing Fig. 2 it is useful to make four remarks: (1) The πN system is not an equal-mass system (as discussed in Secs. II–IV); however, ν in Eqs. (17) is still to be interpreted as the square of the magnitude of the c.m.s. three-momentum; Eqs. (1) and (2) still hold with some modficiations of the ν-plane analyticity of $Y(\nu,l)$ discussed below; these modifications will not concern us in this section. (2) The πN system is not spinless, however, the form of Eqs. (1) and (2) is still valid for the particle-wave amplitudes of definite l. (3) Since $Y(\nu,l)$ is a real analytic function of ν for fixed integer l, its real and imaginary parts are connected appropriately. This will be true of $Y^D(\nu,l)$ calculated from (17) only insofar as the original phase-shift analysis maintained such a connection. The ALMEHED 72 fit contains some degree of energy analyticity through the use of partial-wave dispersions relations, while the AYED 73 fit contains some energy analyticity through the use of energy continuity and resonance-fitting techniques. The reader is referred to the original papers for discussion. Also, it should be noted that the phase conventions of the partial-wave analysis appear in the $Y^D(\nu,l)$ through Eqs. (17). (4) A rough estimate of the error in Y^D is obtained by comparing the Y^D calculated from the AYED 73 "data" (δ's and η's) with the Y^D calculated from the ALMEHED 72 "data." The average difference between the AYED and ALMEHED Y^D values for five data points (energies from 1202 to 1292 MeV) in the P_{33} wave is 0.000 22 GeV^3, while the average difference between the AYED and ALMEHED Y^D values for seven data points (energies from 1822 to 2022 MeV) in the F_{37} wave is 0.027 GeV^7. These differences are shown on Fig. 2 as error bars to provide a crude indication of the uncertainty in the Y^D values calculated from the empirical phase shifts and absorption parameters, and for later use in the fitting.

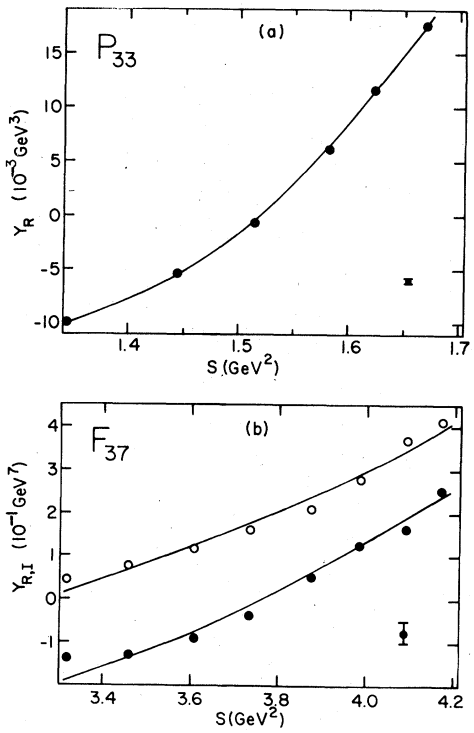

FIG. 2. (a) The solid circles are the function Y_R^D for the πN P_{33} partial wave in the region of the 1232-MeV resonance as calculated from the AYED 73 phase-shift "data" using Eq. (17). The size of the solid circles is an estimate of the error in these data points (see text). The smooth curve is the result of the fit of the γ trajectory model [Eq. (19)] to the P_{33} and F_{37} partial-wave "data." This smooth curve is Y_R^γ as calculated from Eq. (19) using the parameters of the fit (see text). The horizontal axis is the square of the total c.m.s. energy s. (b) The solid circles (open circles) are the function Y_R^D (Y_I^D) for the πN F_{37} partial wave in the region of the 1950-MeV resonance as calculated from the AYED 73 phase-shift "data" using Eq. (17). An estimate of the error in these points is shown in the lower right-hand corner of the figure as an error bar (see text). The smooth curves are the result of the fit of the γ-trajectory model to the P_{33} and F_{37} partial-wave "data." The smooth curve through the solid circles (open circles) is Y_R^γ (Y_I^γ) as calculated from Eq. (19) using the parameters of the fit (see text). The horizontal axis is the square of the total c.m.s. energy s.

Returning now to Fig. 2: to interpret the empirical Y^D values presented in Fig. 2 for the regions of the P_{33} (1232) and F_{37} (1950) resonances it is useful to compare Eq. (2) with the Breit-Wigner resonance form given in Sec. III A, to see how a resonance appears in terms of the $Y(\nu,l)$. Such a comparison yields (ν, s real, l odd integer)

$$Y_R \simeq \frac{\nu_0^{l+1/2}}{x M_0 \Gamma_0}(s - s_0),$$
$$Y_I \simeq \frac{1-x}{x}\nu^{l+1/2} \tag{18}$$

in the vicinity of a resonance of mass M_0, width Γ_0, elasticity x, and angular momentum l. Thus, for a resonance such as the P_{33} (1232) or F_{37} (1950), the real part of Y is linear in s with a zero at the resonance energy s_0, in the Breit-Wigner approximation considered here. (This approximation assumes x, M_0, Γ_0 constants, and no background to rotate or shift the resonance term.) Inspection of Fig. 2 reveals that the real parts Y_R^D in both the P_{33} (1232) and F_{37} (1950) regions are roughly linear in s immediately around the resonance energies, but that they do have significant upward curvature in s representing a departure from the simple Breit-Wigner width $\Gamma = \Gamma_0(\nu/\nu_0)^{l+1/2}$ used here. This departure is well-known, at least in the case of the P_{33} (1232), and has been extensively studied (Ref. 8, pages 103 to 105). For the purposes of this section it is sufficient to observe that the real part of Y^D in the neighborhood of a resonance is empirically a smoothly increasing function of s, with some upward curvature, and with a zero at approximately the resonance energy s_0.

The imaginary part Y_I^D is, of course, zero where the amplitude is purely elastic, either from (18) or from the general theory. Thus, in the region of the P_{33} (1232), Y^D has no imaginary part. In the region of the F_{37} (1950), however, Y_I^D is nonzero and has the general shape in s of Y_R^D with the exception that it does not have a zero in the region. This behavior is consistent with the second of Eqs. (18).

B. γ-trajectory model for Y

The empirically determined $Y^D(s,l)$ values [given in the previous section for the πN P_{33} and F_{37} waves in the regions of the P_{33} (1232) and F_{37} (1950) resonances] can be given a complex angular momentum interpretation by making the hypothesis that the resonance structure observed in the Y is due to the movement of an angular momentum function $\gamma(s)$ in the complex l plane. (In this section and the next two sections the energy s is used instead of ν.) This hypothesis allows the construction of simple models for $Y(s,l)$ in terms of the trajectory and "residue" functions; the γ-trajectory model chosen here is [see (6)]

$$Y^\gamma(s,l) = [l - \gamma(s)]H(s,l), \tag{19a}$$

where the real and imaginary parts of γ and H are parametrized in terms of the energy s as

$$H_R(s,l) = (s - a_7)a_8 c^{2l+1},$$
$$H_I(s,l) = 0,$$
$$\gamma_R(s) = (s - a_1)a_2, \tag{19b}$$
$$\gamma_I(s) = 0 \quad \text{(1232-MeV region only)},$$
$$\gamma_I(s) = (s - a_4)a_5 \quad \text{(1950-MeV region only)}.$$

The three parameters a_1, a_4, a_7 have the dimensions of s, namely GeV^2, while the other three parameters a_2, a_5, a_8 have dimensions GeV^{-2}. The dimensional constant c is set equal to 1 GeV (Y has the dimensions GeV^{2l+1}). The parameters a_2, a_5, a_8 are the slopes of γ_R, γ_I, H_R, respectively. The superscript γ on Y^γ indicates a γ-trajectory model for Y.

The expression (19) is a γ-trajectory model for the dynamical function $Y(s,l)$; the resonance structure in Y (shown, e.g., for πN scattering in Fig. 2) is attributed to the passage of $\gamma(\nu)$ through or near the resonance l value. The significant l dependence in (19) is in the $(l - \gamma)$ factor; it is this factor which causes the vanishing of Y, or of the real part of Y, which is the characteristic signature of a resonance as discussed in Sec. V A above [see also Eq. (13)]. In the model (19), $Y^\gamma(s,1)$ will vanish when $\gamma(s) = 1$, while $Y_R^\gamma(s,3)$ will vanish when $\gamma(s) = 3$. Thus, in the illustration given here, Y^γ of Eq. (19) is used to fit the πN P_{33} wave near the 1232-MeV resonance and the F_{37} wave near the 1950-MeV resonance [$Y^D(s, l=1)$ and $Y^D(s, l=3)$, respectively, of Eq. (17) and Fig. 2]. In other words, the γ trajectory "causes" the 1232-MeV resonance in the P_{33} wave and the 1950-MeV resonance in the F_{37} wave.

There are two reasons why model (19) can be used to fit the partial-wave amplitudes only in the vicinity of a resonance. The first is that the l dependence of the model is only linear and, in general, one would not expect to be able to extrapolate very far in the l plane without including higher powers of l. The second, and more important reason, is that the πN partial-wave amplitudes as determined from the phase-shift analyses contain more than one resonance per partial wave. Model (19) contains only one resonance in a given partial wave, and so is unsuited for fitting energy regions of the partial wave far from the resonance where background and a second resonance become important. The energy region fitted could be widened by adding a second trajectory to the model and, possibly, a background term, but that would be considerably beyond the scope of the present illustration.

Before discussing the fitting of the model to the data of Fig. 2 it is useful to make five comments: (1) The model (19) describes Y as essentially linear in both l and s (ignoring the dimensional factor c^{2l+1}); this is clearly not theoretically correct for all l, s values, the model is intended only as a simple approximation for use in restricted regions of the angular momentum and energy planes. (2) The Y^γ as given in (19) does not have the correct energy-plane analytic structure, e.g., its real and imaginary parts are not appropriately connected. The simplicity and flexibility of expressions (19) for γ and H is desirable for the simple illustrative use here, but for a more detailed phenomenological study of γ and H it might be useful to incorporate a more correct analytic structure in the model for Y. (3) The amplitude $A(s,l)$ constructed by using (19) in (2) has the correct elastic kinematic cut. Thus, e.g., a real Y^γ results in an $A(s,l)$ on the Argand circle. The model contains s-channel unitarity. In addition, the amplitude $A(s,l)$ has the correct threshold energy dependence for both the real and imaginary parts. (4) The choices $\gamma_I = 0$ and $H_I = 0$ near 1232 MeV made in (19) are motivated by the fact that in the region of the P_{33} (1232) resonance the P_{33} wave is purely elastic so that Y^γ is real. (5) The choice $H_I = 0$ near 1950 MeV in (19) is motivated by the desire to keep the model as simple as possible. In general, above ν_{inel} the imaginary part of H will be nonzero. It is shown below, however, that a good fit to the data is possible with $H_I = 0$. In more detailed studies of γ and H it would be desirable to allow H to have a nonvanishing imaginary part above ν_{inel}.

C. Fit to the πN data

The γ-trajectory model (19) was fitted to the AYED 73 Y^D values calculated from Eqs. (17) and shown in Fig. 2 using a standard χ^2 minimization program. The data consist of six points in the P_{33} wave and sixteen in the F_{37} wave which were fitted by adjusting the six parameters a_i of the model. The "errors" used were those discussed in Sec. V A and shown in Fig. 2. Since these are not "true" errors, the χ^2 is not a true χ^2, but rather an estimate of the χ^2; I refer to this as the effective χ^2. The main usefulness of the "errors" is in determining the relative weight in the fit of the P_{33} and F_{37} data points. Since the P_{33} "errors" are approximately a factor of 100 smaller than the F_{37} "errors," the P_{33} points play a dominant role in the fit in spite of the fact that they number only 6 versus the 16 points of the F_{37} wave. Nevertheless, as will be discussed below, the F_{37} points are well fitted. The effective χ^2 for the fit, shown in Fig. 2, is 15.9 for the 16 degrees of freedom indicating a reasonable fit. That the fit is acceptable can also be seen by inspection of Fig. 2 which shows both the data and the fitted model curves. The parameter values for the fit are $a_1 = 0.04$ GeV^2, $a_2 = 0.89$ GeV^{-2}, $a_4 = 3.25$ GeV^2, $a_5 = 0.65$ GeV^{-2}, $a_7 = 1.05$ GeV^2, $a_8 = -0.21$ GeV^{-2}. No attempt was made to determine the errors in these parameter values because of the crudeness of the model and because of the lack of a true χ^2. However, as will be discussed below, some parameters are determined more precisely than others.

Because of the simple nature of the model, in particular, because of the assumption $H_I = 0$, not all of the parameters are involved in fitting all of the 22 data points. As is seen in Eq. (19) the model uses $\gamma_R(a_1, a_2)$ and $H_R(a_7, a_8)$ to fit the Y_R^D points in both the P_{33} and P_{37} waves, while $\gamma_I(a_4, a_5)$ and $H_R(a_7, a_8)$ are used to fit the Y_I^D points in the F_{37} wave. Because of this "division of labor" among the parameters, and because of the much smaller errors (and hence greater weight) of the P_{33} data points, the parameters are determined *approximately* as follows. The P_{33} data points determine three of the four γ_R and H_R parameters e.g., a_1, a_7, and a_8. The fourth parameter, a_2 of γ_R (the slope of the trajectory), is then determined by the eight F_{37} points of Y_R^D. Since γ_R and H_R are now determined, this leaves only γ_I free to fit the eight Y_I^D points of the F_{37} waves; this then determines a_4 and a_5. The γ_R and H_R parameters are more precisely determined than the γ_I parameters because they occur in both partial waves, and because of the smaller P_{33} "errors."

Speaking more physically, the real part of the trajectory γ_R can be thought, e.g., as being primarily determined by the resonance masses 1232 and 1950 MeV; these are the points the where Y_R^D vanishes for the P_{33} and F_{37} waves, respectively. This determination of γ_R by the resonance masses is, of course, what occurs with α_R in the more usual cross-channel data analyses involving the Regge trajectory α. The value of the γ trajectory slope found here, 0.89 GeV^{-2}, is consistent with the usual slope found for the Δ Regge trajectory 0.9 GeV^{-2} (see Refs. 3 and 5).

Perhaps the most notable feature of the fit is that the F_{37} wave is well fitted in spite of the fact that the P_{33} wave "errors" are a factor of 100 smaller than the F_{37} "errors." The effective χ^2 of 15.9 divides into 5.7 for the six Y^D P_{33} points, 6.2 for the eight Y_R^D F_{37} points, and 4.0 for the eight Y_I^D F_{37} points. This division indicates that the contributions to χ^2 come approximately equally from the P_{33} and F_{37} parts of the fit. Thus there appears to be reasonable consistency of the model with the data.

D. Discussion of γ,α trajectories

In the complex l plane the γ trajectory [as determined empirically in the previous sections from the P_{33} (1232) and F_{37} (1950) data] follows the Rel axis until about the point $l=2.7$ where it leaves the Rel axis in a straight line developing a positive imaginary part. Thus this simple phenomenological γ trajectory is similar to the schematic representation of a γ trajectory given earlier in Fig. 1(a): It is real in the elastic [P_{33} (1232)] region and becomes complex in the inelastic [F_{37} (1950)] region. This empirical γ trajectory and the model fit to the data are reasonable so it is natural to ask if an equally simple phenomenological analysis can be carried through for the α trajectory. Unfortunately the answer to this question appears to be no as can be seen from the following discussion.

An α-trajectory model analogous to model (19) can be constructed by using $Y=(l-\gamma)H$ from (19), plus definitions (3) and (4). The result is

$$Y=(l-\alpha)H-(-\nu)^{\alpha+1/2}, \tag{20}$$

where H is independent of l except for a dimensional factor [see (19)], and where a similar dimensional factor is suppressed in the $(-\nu)^{\alpha+1/2}$ term. Thus, apart from the dimensional factors, this model is linear in l as is model (19).

The α model (20) for Y is more complicated phenomenologically than the γ model (19) for two main reasons. First in the elastic region where Y and H are real the α trajectory is complex. Thus the imaginary parts of the αH and $(-\nu)^{\alpha+1/2}$ terms must exactly cancel. While it is of course possible to arrange α and H to provide the necessary cancellation, it is awkward to construct a real function from complex functions. This situation is in contrast to the γ model (19) where γ and H are real in the elastic region so that the real Y is easily parametrized. The second complication of (20) is in the form of its dependence upon α in the "kinematic" term $(-\nu)^{\alpha+1/2}$. This kinematic term is essentially oscillatory in its dependence upon α. A fit of model (20) was made to the πN P_{33} and F_{37} data described above, and it was found that α_I became negative for energies above ~1400 MeV. This bad result is traceable to the oscillatory character of $(-\nu)^{\alpha+1/2}$ which causes α_I to change sign as α_R increases.

In summary a satisfactory fit of the α model (20) to the data was not possible. However, this does not imply that the γ trajectory is in general superior phenomenologically to the α trajectory. The models chosen for comparison are both overly simple in their l dependence, and it might be that the l dependence of the "true" Y is such that the α trajectory is equal or superior to the γ trajectory in a simple phenomenological sense.

VI. CONCLUSION

In conclusion I make six observations. First, using the technique of Froissart[16] one can formally remove the remaining right-hand cut from $Y(\nu,l)$ and thus define a further-reduced trajectory function which is real for all physical values of energy $0\leq\nu\leq+\infty$. This procedure is, however, formal because the imaginary part of Y is essentially dynamical in character and thus unknown. Second, Y and γ still contain so-called inelastic kinematics; in principle these are present both below and above ν_{inel}. My view here is that inelastic kinematics are (again) essentially dynamical in character so that "kinematics-free" is more precise with the reservations expressed in Sec. III. Third, since the kinematic term present in α is gone from γ, it is "easier" for γ_R to be linear in the energy, especially at threshold [see, e.g., (14)]. α_R cannot be linear in energy at threshold except for special values of $\alpha(0)$. Fourth, since the kinematic term $(-\nu)^{l+1/2}$ vanishes at threshold it appears likely that $\gamma(0)=\alpha(0)$. This can be proven in simple models for $Y(\nu,l)$. Fifth, it would be useful to examine the very high-energy behavior of $\gamma(\nu)$, and compare this behavior with that of the Regge trajectory $\alpha(\nu)$. Sixth, much of the discussion in this paper has emphasized the direct channel at low energy. For the case where there is a trajectory exchanged in the cross channel, and one is interested in high energies, the traditional α trajectory may retain significant advantages over the γ trajectory because it is a pole of the amplitude while γ is not. However, this has not been investigated.

In summary, I have attempted to show that it is possible to define other complex angular momentum trajectories beside the usual Regge trajectory α, and that, in certain situations, these provide a useful alternative to α.

ACKNOWLEDGMENT

This work was supported by the U. S. Department of Energy, Office of Energy Research, Division of High Energy and Nuclear Physics under Contract No. W-7405-eng-82. I am indebted to my associates for many helpful conversations, in particular to J. P. Jarrett, T. L. Zimmerman, B.-L. Young, D. K. Ross, and H. B. Crawley. In addition, J. P. Jarrett provided extensive help with the fitting program, and T. A. Lasinski and R. L. Kelly of the Particle Data Group provided tapes of the recent πN phase-shift analyses, and useful discussion of these analyses.

APPENDIX A

In this Appendix I discuss the relation of the Regge trajectory α and the γ trajectory of this paper to the "maximal-amplitude trajectory" (MAT) of Tani and Inokuti (TI).[13] In Sec. II of this paper the trajectories α and γ are defined as poles of the S matrix and of a function $Y^{-1}(\nu,l)$, respectively [Eqs. (4) and (5)]. In TI the MAT is defined above threshold as a pole of the K matrix. The MAT and the γ trajectory above threshold are different functions as can be seen from the fact that Y^{-1} is not the K matrix. The relation between Y^{-1} and the S matrix follows from Eq. (2), and is also given by De Alfaro and Regge in Eq. (5.27) of their book[1] (recall $Y = e^{-i\pi l}Z$; Ref. 12); the relation is

$$Z^{-1} = (e^{i\pi l}Y)^{-1} = (i\nu^{l+1/2})^{-1}\frac{S-1}{S-e^{2i\pi(l+1/2)}},$$

while the corresponding relation between K and the S matrix is[17]

$$K = (i\nu^{l+1/2})^{-1}\frac{S-1}{S+1}.$$

This definition of K results in K being proportional to $\tan\delta$ [see Eq. (2.10) of TI and Ref. 17]. For the purposes of the present discussion the significant difference between Y^{-1} and K is the term $\exp[2i\pi(l+\frac{1}{2})]$. As discussed in De Alfaro and Regge this term is essential to making Y single valued in energy near the elastic threshold; thus the relatively simpler analytic properties of Y follow from its precise definition. In summary, above threshold Y^{-1} and the K matrix are different quantities, and the γ trajectory and the MAT are not the same functions.

Below threshold α and γ continue to have the same definitions they had above threshold so that α and γ are analytic functions "through" the threshold region. In contrast, in TI two different Green's functions are used for the above [TI, Eq. (2.4)] and below [TI, Eq. (2.21)] threshold cases. What is done in TI is to match the Regge trajectory α below threshold (with its definition in terms of S) to the MAT above threshold (with its definition in terms of K); this does not result in a complex angular momentum trajectory which is an analytic function of the energy in the neighborhood of the elastic threshold. In conclusion, the γ trajectory and the TI trajectory are different quantities above and below threshold.

Ross and Shaw[18] observe that because the K matrix is defined in terms of principal-value wave functions, the K matrix elements calculated above a threshold and continued below the threshold are not the same as the K matrix elements calculated below the same threshold [see their Footnote 1 and the discussion following their Eq. (37); see also Ref. 17]. Thus, care must be exercised when using the K matrix "across" a threshold. It is interesting to note that in spite of the fact that Y^{-1} and K appear similar in form, they are quite different quantities, and that when considered as a function of the energy, Y is the simpler function, especially near the elastic threshold. It is the fact that Y is single-valued in energy at threshold that makes the γ trajectory real for physical energies in the neighborhood of the threshold.

APPENDIX B

Equation (14) of Sec. IV A shows that $\gamma(\nu)$ is real and analytic in ν near threshold $\nu = 0$. In addition, it was stated in Sec. IV A that $\gamma(\nu)$ is a real analytic function of ν, and so, that one might expect γ to be real for $0 < \nu < \nu_{\text{inel}}$ unless two γ trajectories collide. In this appendix we examine the possibility of trajectory collision in the region $0 < \nu < \nu_{\text{inel}}$ using the relativistic phase shift $\delta(\nu,l)$.

By combining Eqs. (1) and (2) one can obtain

$$Y(\nu,l) = \nu^{l+1/2}[\cos\pi l\cot\delta(\nu,l) + \sin\pi l]. \qquad \text{(B1)}$$

Using this expression with definition (5) for $\gamma(\nu)$ yields a relation between γ and the relativistic phase shift δ:

$$\pi\gamma(\nu) = \delta(\nu,\gamma(\nu)) + (n+\tfrac{1}{2})\pi \qquad \text{(B2)}$$

where n is an integer. A way to visualize how γ trajectories are obtained from (B2) for $\nu > 0$ is to imagine that the straight line $\pi l - (n+\frac{1}{2})\pi$ and the curve $\delta(\nu,l)$ are plotted versus l (for fixed ν, n), on the same graph. The point of intersection of the straight line and the curve is a solution of (B2) and thus gives the value of γ for the given n and ν. There are two ways γ trajectories might collide: first, two trajectories with different n values might intersect, and second, two trajectories with the same n value might collide; I consider these two possibilities in order.

Two γ trajectories with different n values (say n' and n'') arise from the intersections of the two straight lines $\pi l - (n'+\frac{1}{2})\pi$ and $\pi l - (n''+\frac{1}{2})\pi$ with the curve $\delta(\nu,l)$. The only way these two intersections can fall at the same value of l is if the curve $\delta(\nu,l)$ has an infinitely negative slope in l so that δ can intersect the two straight lines at the same l value. But, for $\nu > 0$, $\partial\delta/\partial l > -\infty$ so that this source of γ trajectory collision is eliminated.

The second possible type of γ trajectory collision is for two γ trajectories with the same value of n to collide. If the slope of $\delta(\nu,l)$ (again as a function of l for fixed ν) exceeds π, then the δ curve can intersect the straight line $\pi l - (n+\frac{1}{2})\pi$ by

rising through it. Later, for a larger value of l, δ can again intersect the (same) straight line by *falling* through it. Thus, two γ trajectories could arise from the same line $\pi l - (n+\frac{1}{2})\pi$; these two trajectories would collide for a higher value ν when the δ curve becomes lower. In potential scattering, such a situation where two γ trajectories have the same n value is excluded for $\nu > 0$ because of the bound[19] on the derivative of δ: $\partial\delta/\partial l < \pi/2$, and thus this type of collision is not possible. In relativistic scattering I am not aware of a similar bound on $\partial\delta/\partial l$, but it is likely that such a bound exists if the potential-scattering result is a rough guide as to what to expect in relativistic scattering. In conclusion, a bound $\partial\delta/\partial l < \pi$ on the relativistic phase shift for $\nu > 0$ will prevent γ trajectory collisions for $\nu > 0$ (if such a bound exists); this bound is considerably weaker than the known potential-scattering bound $\partial\delta/\partial l < \pi/2$.

[1]V. De Alfaro and T. Regge, *Potential Scattering* (North-Holland, Amsterdam, 1965); also A. Bottino, A. M. Longoni, and T. Regge, Nuovo Cimento 23, 954 (1962). The function Z of these studies is related to the Y of Eq. (2); see Ref. 12.

[2]S. C. Frautschi, *Regge Poles and S-Matrix Theory* (Benjamin, New York,, 1963).

[3]P. D. B. Collins and E. J. Squires, *Regge Poles in Particle Physics*, Springer Tracts in Modern Physics, Vol. 45 (Springer, New York, 1968).

[4]R. G. Newton, *The Complex j-Plane* (Benjamin, New York, 1964).

[5]V. D. Barger and D. B. Cline, *Phenomenological Theories of High Energy Scattering* (Benjamin, New York, 1969).

[6]S. Almehed and C. Lovelace, Nucl. Phys. B40, 157 (1972). This pion-nucleon elastic-phase-shift analysis is referred to as ALMEHED 72 by the Particle Data Group.

[7]R. Ayed, P. Bareyre, and Y. Lemoigne, talk given at the XVI International Conference on High Energy Physics, Chicago-Batavia, Ill., 1972 (unpublished). This phase-shift analysis is referred to as AYED 73 (or 74) by the Particle Data Group.

[8]Particle Data Group, Phys. Lett. 39B, 1 (1972).

[9]Particle Data Group, Rev. Mod. Phys. 45, S 1 (1973).

[10]Particle Data Group, Phys. Lett. 50B, 1 (1974).

[11]S. Mukherjee, Phys. Rev. 160, 1546 (1967).

[12]A. O. Barut and D. E. Zwanziger, Phys. Rev. 127, 974 (1962); this paper is referred to as BZ in the text. The function Y of BZ and Eq. (2), and the Z of Ref. 1 are related by $Y = Z\exp(-i\pi l)$. The properties of Y are discussed in terms of the Mandelstam representation in BZ, while the properties of Z follow from the Schrödinger equation in Ref. 1. (The logarithm cut is along the negative real axis.)

[13]S. Tani and M. Inokuti, J. Chem. Phys. 61, 4422 (1974), and references therein. This paper is referred to as TI.

[14]J. R. Taylor, Phys. Rev. 127, 2257 (1962).

[15]E. Hille, *Analytic Function Theory* (Ginn, New York, 1959), Vol. 1.

[16]M. Froissart, Nuovo Cimento 22, 191 (1961).

[17]R. Levi Setti and T. A. Lasinski, *Strongly Interacting Particles* (University of Chicago, Chicago, 1973).

[18]M. H. Ross and G. L. Shaw, Ann. Phys. (N.Y.) 9, 391 (1960).

[19]See, e.g., J. R. Taylor, *Scattering Theory* (Wiley, New York, 1972).